ARTICLE

Electrochemical and Structural Characterization of Polymer Gel Electrolytes Based on a PEO Copolymer and an Imidazolium-Based Ionic Liquid for Dye-Sensitized Solar Cells

Flavio S. Freitas, Jilian N. de Freitas, Bruno I. Ito, Marco-A. De Paoli, and Ana F. Nogueira*

Laboratório de Nanotecnologia e Energia Solar (LNES), Universidade Estadual de Campinas, UNICAMP, P.O. Box 6154, 13083-970, Campinas SP, Brazil

ABSTRACT Polymer electrolytes based on mixtures of poly(ethylene oxide-*co*-propylene oxide) and 1-methyl-3-propyl-imidazolium iodide (MPII) were investigated, aiming at their application in dye-sensitized solar cells (DSSC). The interactions between the copolymer and the ionic liquid were analyzed by infrared spectroscopy and ^{1}H NMR. The results show interactions between the ether oxygen in the polymer and the hydrogen in the imidazolium cations. The ionic conductivities, electrochemical behaviors, and thermal properties of the electrolytes containing different concentrations of MPII were investigated. The electrolyte containing 70 wt % MPII presented the highest ionic conductivity (2.4×10^{-3} S cm^{-1}) and a diffusion coefficient of 1.9×10^{-7} cm^2 s^{-1}. The influence of LiI addition to the electrolytes containing different concentrations of MPII was also investigated. The DSSC assembled with the electrolyte containing 70 wt % MPII showed an efficiency of 3.84% at 100 mW cm^{-2}. The stability of the devices for a period of 30 days was also evaluated using sealed cells. The devices assembled with the electrolyte containing less ionic liquid showed to be more stable.

KEYWORDS: dye-sensitized solar cells • polymer gel electrolyte • ionic liquid • stability

INTRODUCTION

Since Grätzel's pioneering work on efficient dye-sensitized solar cells (DSSC) (1), this kind of technology has attracted significant attention from the scientific and industrial community. These devices were usually assembled with a liquid electrolyte, but the presence of this liquid component was considered a drawback, especially considering the long-term stability of the devices. One alternative to the liquid electrolyte is the use of polymer hole conductors (2) or polymer electrolytes (3−11). The combination of a coordinating polymer and a suitable salt has the advantages of their solid state and their conducting nature. However, the increased viscosity leads to a low and limited ionic transport (12) and an insufficient penetration of the electrolyte into the nanoporous titania photoelectrode (13). Thus, the devices using pure polymers present lower values of current, fill factor, and efficiency when compared to DSSC assembled with liquid electrolytes (3).

Considering this, the addition of high-boiling-point organic solvents or low-molar-mass polymers has made polymer gel electrolytes more attractive. Polymer gel electrolytes possess higher ionic conductivity, comparable to those observed for liquid electrolytes. Besides, it has been demonstrated that the amount of salt dissolved in the electrolyte can be increased after addition of the organic solvent, leading to a more efficient reduction of the dye cation in the DSSC (10). However, the mechanical properties are poorer than those of the pure polymer electrolyte, and although the gel electrolyte has lower viscosity, it does not guarantee a complete filling of the titania photoelectrode. Therefore, even in the case of gels, special techniques such as the deposition of the electrolyte under a vacuum should be employed to improve the devices' efficiency (14). An elegant alternative was proposed by Kang and coworkers (15), where polymer electrolytes based on a low-molar mass poly(ethylene glycol) with special terminal functional groups were combined with an ionic liquid and, in the liquid state, introduced into the TiO_2-sensitized photoelectrode. After drying, the hydrogen bonding promoted between the terminal groups yields a solid-state film, resulting in a solid-state DSSC with high efficiency because of the better penetration of the electrolyte into the titania film.

In this context, the use of room temperature ionic liquids (IL) is an interesting alternative to make gel electrolytes. These ionic liquids were first investigated in 1951 (16). Since then, their application in electrochemical devices has been exploited because of their attractive properties, such as chemical and thermal stability, nonvolatility, and high ionic conductivity at room temperature. DSSCs with efficiencies above 7% using ionic liquid-based electrolytes have been reported (17−19).

* Corresponding author. E-mail: anaflavia@iqm.unicamp.br. Fax: +55 19 35213023. Tel: +55 19 35213029.

Received for review September 2, 2009 and accepted November 9, 2009

DOI: 10.1021/am900596x

Published on Web 11/25/2009

Most of the ILs present a wide electrochemical stability range and high viscosity, and they can act as solvent (20) or gellators to liquid electrolytes (21, 22) or be combined with solid materials, such as a polymer or an inorganic nanoparticle (23), to give gels (24−27). In fact, considering DSSC with polymers and IL, at least two different approaches have been reported in the literature: (i) the combination of polymers or copolymers with IL, to improve both the ionic conductivity and the mechanical properties of the electrolyte (28−32); and (ii) the polymerization of ionic liquids or the insertion of IL molecules into a polymer chain, in order to make ionic conducting polymers (33 –36).

The incorporation of an IL in the polymer electrolyte may substitute the addition of other iodide-based salts, such as LiI, NaI, or KI, because this material can be used as a source of iodide ions in the solar cells. Also, large amounts of IL can be dissolved in the polymer medium because of the interaction of the imidazolium cation with the oxygen atoms present in the ethylene oxide units (37), and therefore, the number of charge carriers can be increased. In addition, for the ionic liquid system, the change in open circuit voltage (V_{oc}) is negligible because of the larger size of cations (38) and the good charge delocalization can well-restrain the recombination reaction (23). Thus, in the case of bulk cations, which cannot penetrate into the dye molecular layer, or intercalate, the triiodide anion, as an electron acceptor will experience a repulsive force to penetrate the dye layer (39).

Although many papers have shown the improvement in DSSC performance using electrolytes that combine IL with several different types of materials, only a few papers present the investigation of an electrolyte based solely on the IL as ionic source. This work sets forth the characterization of polymer electrolytes based on the combination of a copolymer of ethylene oxide and propylene oxide and 1-methyl-3-propyl-imidazolium iodide, with and without the addition of LiI, and their application in dye-sensitized solar cells.

EXPERIMENTAL SECTION

Preparation of the Polymer Gel Electrolytes. Polymer electrolyte solutions were prepared by dissolving 0.3 g of poly(ethylene oxide-*co*-propylene oxide), P(EO-PO), with a comonomer ratio of 77/23 and 20, 40, or 70 wt % of ionic liquid 1-methyl-3-propyl-imidazolium iodide (MPII, Solaronix) in acetone. The solutions were stirred for 24 h and I_2 was then added to obtain a MPII:I_2 molar ratio of 10:1. All the materials were used as received. The copolymer was furnished by Daiso Co. Ltd. (Osaka, Japan), and the molar mass reported by the supplier was $\sim 1 \times 10^6$ g mol^{-1}. The electrolyte solutions were kept under stirring for 72 h before the measurements.

Ionic Conductivity Measurements. The polymer solutions were dropped onto stainless steel disks, using adhesive tape to control thickness, and the solvent was evaporated in an air atmosphere for 48 h. After this period, they were kept in a desiccator with P_2O_5 to remove excess moisture. The systems were sandwiched using a second stainless steel disk, and dried under vacuum for 72 h before the measurements.

The electrochemical impedance spectroscopy (EIS) measurements were done by placing the samples in a Mbraun drybox ([H_2O] < 1 ppm, under an argon atmosphere) and using an Eco Chimie-Autolab PGSTAT 12 potentiostat with a FRA module. The frequency range analyzed was 1×10^0 to 1×10^6 Hz with amplitudes of ±10 mV over the open circuit potential. The ionic conductivity values were calculated from the Nyquist plots.

Instruments and Measurements. The electrochemical properties of the polymer gel electrolytes were further investigated using a symmetric thin-layer cell, where the polymer electrolyte film was placed between two Pt-coated transparent conductive oxide-coated glass (TCO) electrodes with an active area of 1 cm^2. The film thickness ($\sim$60 μm) was controlled using adhesive tape. EIS measurements were performed using the frequency range from 1×10^{-4} to 1×10^6 Hz using conditions as described in ionic conductivity measurements.

The thermal properties of the polymer gel electrolytes were characterized by differential scanning calorimetry (DSC) using a TA Instruments Thermal Analyzer model 2100, coupled to a TA 2100 Data Analysis System, under a nitrogen flow rate of 100 mL min^{-1} and according to the following procedure: (1) heating from room temperature to 100 at 20 °C min^{-1}; (2) isotherm for 5 min at 100 °C; (3) cooling to −100 at 10 °C min^{-1}; (4) second heating to 100 °C at a heating rate of 10 °C min^{-1}. The results presented here are based on the second heating step.

^{1}H NMR spectra were recorded using a Bruker 250 spectrometer operating at 250 MHz, employing deuterated chloroform as solvent and tetramethylsilane (TMS) as standard (zero).

Dye-Sensitized Solar Cells. DSSC were assembled using TCO electrodes (Hartford glass, $R_s \approx 10\ \Omega\square$) as substrates for both photoelectrode and counter-electrode (CE). CE were prepared by spreading a 50 mmol L^{-1} solution of H_2PtCl_6 in isopropanol onto the TCO substrate, and then firing at 350 °C for 20 min, yielding semitransparent Pt-based CE. For preparation of the oxide photoelectrodes (active area of 0.25 cm^2), an aliquot of a commercial TiO_2 suspension (Ti-Nanoxide T, Solaronix) was spread onto the TCO by the "doctor blading" technique, using 3 layers of adhesive tape (Scoth Magic Tape, 3M; thickness $\sim$50 μm) to control the film thickness. After drying in air for 5 min, the films were heated at 350 °C for 15 min and at 450 °C for 30 min. The $TiCl_4$ treatment was applied as previously described (40) by soaking in a 50 mM $TiCl_4$ solution for 30 min at 70 °C, followed by a water rinse and an identical heat treatment. This procedure gave TiO_2 films with 7 μm of thickness, as measured in an Alpha-Step profilometer. The electrodes were immersed in a 0.15 mmol L^{-1} solution of the sensitizer tetrabutylammonium *cis*-bis(isothiocyanate)bis(2,2-bipyridyl-4,4-dicarboxylate)-ruthenium(II) (N719, Solaronix) in absolute ethanol for 18 h. After that, the electrodes were rinsed with ethanol and dried in air for 5 min. The devices were sealed by Himilan (Mitsui-Dupont Polychemicals) and the internal space was filled with the electrolyte solution using a vacuum pump. Afterward, the solar cells were heated to 100 °C under a vacuum to remove acetone. This procedure was repeated several times until a uniform layer of the polymer gel electrolyte was obtained. The hole on the counter electrode glass substrate was sealed with a cover glass and Himilan film.

The DSSC were characterized under irradiation of an Oriel Xe (Hg) 250 W lamp with AM 1.5 filter, used to simulate the solar spectrum. The light intensity was adjusted using a Newport Optical Power Meter. Current−potential curves (I−V curves) were obtained using linear sweep voltammetry at 1 mV s^{-1} using an Eco Chimie-Autolab PGSTAT 10 potentiostat.

RESULTS AND DISCUSSION

Ionic Conductivity Measurements. Figure 1A displays the plots of ionic conductivity of the electrolyte based on P(EO-PO) as a function of MPII content. The maximum amount of 70 wt % MPII was chosen because this is the maximum concentration for good mechanical properties, as

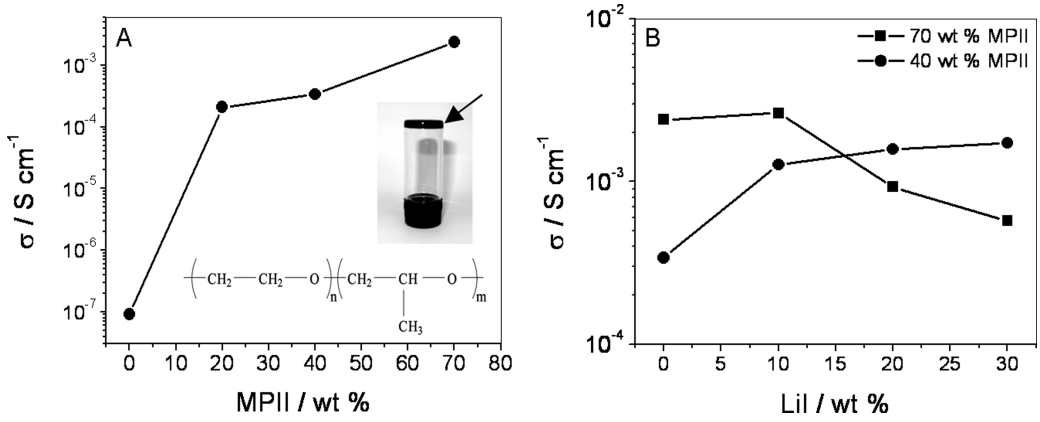

FIGURE 1. Ionic conductivity plots for the electrolytes containing P(EO-PO) and different concentrations of MPII (A) before and (B) after addition of LiI. The LiI content is expressed as a function of MPII + P(EO-PO) weight. The insets show the structure of the copolymer P(EO-PO), where $n = 0.77$ and $m = 0.23$, and the vessel containing the electrolyte with 70 wt % MPII upside down, indicating lack of fluidity of the system in these conditions.

can be seen by the inset showing the vessel upside down with no fluidity. Since the solid nature of the electrolyte is one of the advantages of working with this system, samples containing more than 70 wt % MPII were not investigated.

For the electrolytes investigated here, the addition of 20 or 40 wt % of MPII to the polymer leads to ionic conductivities values ($\sim 1 \times 10^{-4}$ S cm^{-1}) comparable to those obtained for gel electrolytes based on a combination of polymer, salt and additives (5, 9, 10). When the amount of MPII is increased to 70 wt %, the conductivity reaches 2.4×10^{-3} S cm^{-1}, which is comparable to the values obtained for a solution of I^- ions in organic media (41). The ionic conductivity values obtained here are much higher than those reported for polymer electrolytes based on PEO or poly(ethylene glycol) with ionic liquids ($\sim 1 \times 10^{-5}$ S cm^{-1}) (15, 28). This high ionic conductivity may originate from the high concentration of free I^- ions in the electrolyte because of the interaction between the oxygen atom of the copolymer units and the imidazolium cations. Such interaction will be carefully discussed in the next section. Besides, the high concentration of free iodides in the presence of iodine can lead to the formation of polyiodides as showed in our previous work (42). These species do not obey the fundamental Stokes−Einstein equation ($D = kT/6\pi r\eta$), suggesting a new conductive pathway (electronic conductivity) by the well-known Grotthus relay-type mechanism (25, 43, 44). As demonstrated by Grätzel and coworkers (25), the product $D\eta$ is dependent on the electrolyte composition and it is responsible for the higher diffusion than expected from polyiodide dimensions.

Figure 1B presents the plots of ionic conductivity for the electrolytes containing P(EO-PO) and 40 or 70 wt % of MPII, after addition of different amounts of LiI. For the electrolyte containing 40 wt % MPII, an increase in the ionic conductivity is observed when 10 wt % LiI is added and the conductivity reaches $\sim 2 \times 10^{-3}$ S cm^{-1} after addition of 20 wt % LiI. In these cases, probably there are free oxygen atoms in the polymer chains, which can coordinate the Li^+ cations, and therefore contribute to an effective dissociation of the salt, leading to an increase in the number of free charge carriers in the system.

The addition of 10 wt % LiI to the electrolyte containing 70 wt % MPII does not lead to any improvement in the ionic conductivity. Contrarily, the addition of higher amounts of LiI even decreases the conductivity values. Under these conditions, the system shows similar effect observed to polymer electrolytes with poly(ethylene oxide) and poly(propylene oxide), where the dissolution of salt increases the viscosity due the formation of transient cross-linking points between ether oxygen atoms and ions (45). Thus, the ionic mobility (and also the conductivity) is diminished as a consequence of an increase in the viscosity.

The concentration of I^- in the electrolyte containing 40 wt % MPII is ~ 1.7 mmol g^{-1}, whereas in the electrolyte containing 70 wt %, such concentration is ~ 2.5 mmol g^{-1}. The addition of 20 wt % LiI to the former increases the concentration of iodide to 2.5 mmol g^{-1}, similar to the condition presented by the system with 70 wt % MPII. However, the ionic conductivity observed is slightly lower, possibly because the Li^+ and I^- ions are not mobile because of the high concentration of ionic species.

Thermal Analysis. Figure 2 shows the DSC curves for pure P(EO-PO) copolymer and MPII samples and for the electrolytes containing P(EO-PO) with 20, 40, or 70 wt % of MPII. In the region investigated, the pure copolymer presents a glass transition temperature (T_g) at − 66 °C and a crystallization peak followed by a broad melting transition between −30 and 50 °C. The estimated melting enthalpy is 15 J g^{-1}, corresponding to a crystallinity degree of 6%. The pure ionic liquid presents only a fusion at − 68 °C. For the electrolyte containing 20 wt % MPII polymer crystallization and melting transitions can still be observed, but the crystallinity degree is estimated to be only 2% in this case. For the electrolytes containing higher amounts of MPII, no crystallization or melting transition are observed, indicating that the MPII is interacting with the copolymer. For all the binary mixtures (MPII + P(EO-PO)), the T_g is observed at -56 ± 1 °C, independent of the ratio between the ionic liquid and the copolymer. This result suggests that there is a loss in the polymer chain mobility after addition of the ionic liquid,

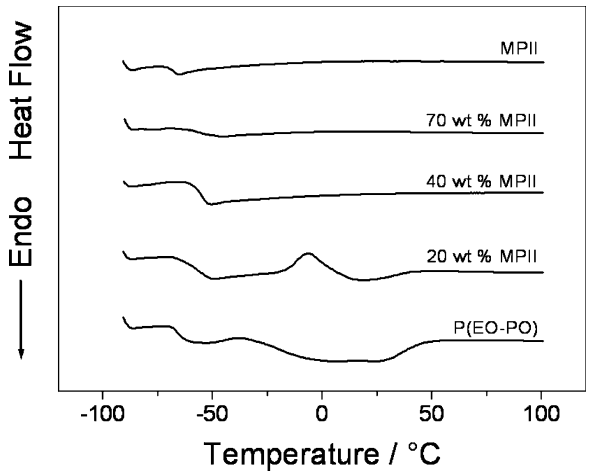

FIGURE 2. DSC analysis of P(EO-PO), MPII, and mixtures containing different ratios of these two materials, under a nitrogen flow rate of 100 mL min^{-1} and a heating rate of 10 °C min^{-1}. The results reported here are based on the second heating step.

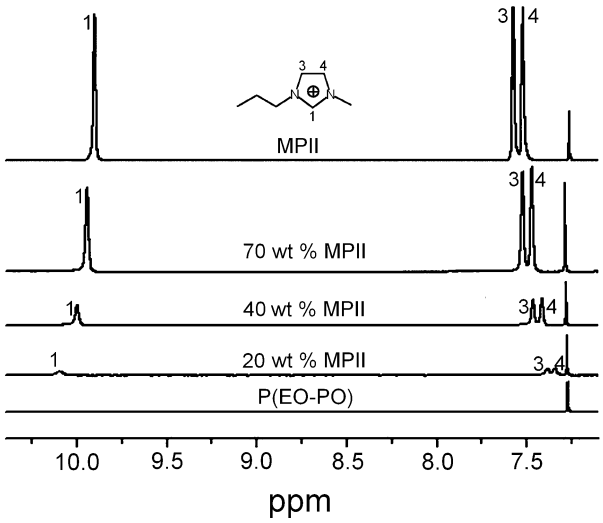

FIGURE 3. ^{1}H NMR spectra of P(EO-PO), MPII, and mixtures containing different ratios of these materials.

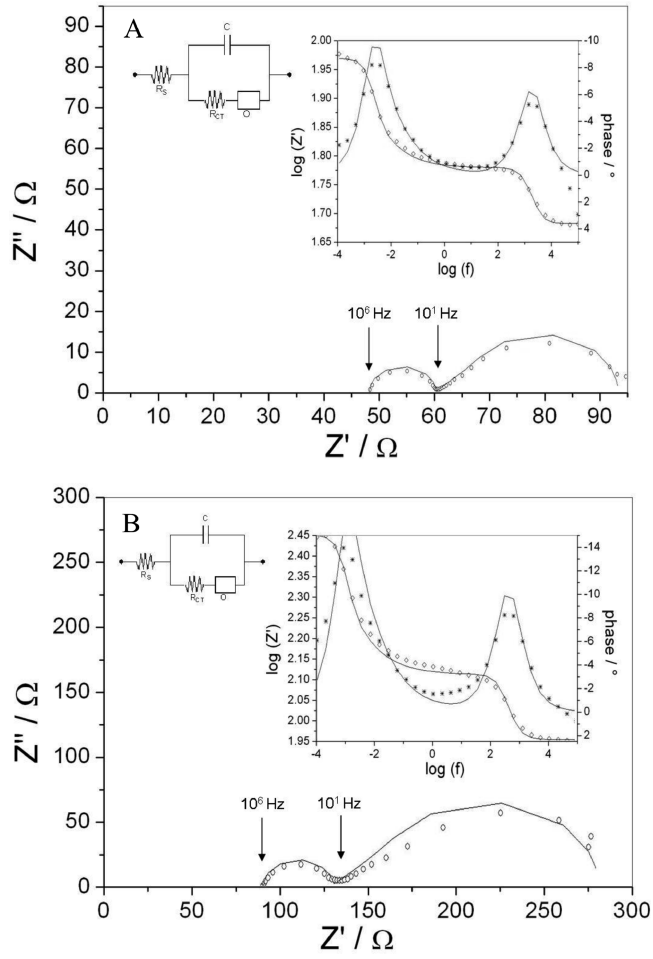

FIGURE 4. Nyquist diagrams obtained from EIS experiments for polymer electrolyte films containing P(EO-PO) and (A) 70 and (B) 40 wt % MPII, sandwiched between planar platinum electrodes. The experimental data are represented by symbols and the solid lines correspond to the fit using the equivalent circuit shown in the inset.

possibly caused by an ion−dipole interaction between the oxygen heteroatoms in the polymer and the imidazolium cations.

To further characterize the interaction between the copolymer and the ionic liquid, we employed FTIR measurements (see the Supporting Information). The addition of MPII to the polymer P(EO-PO) leads to a shift in the band attributed to the C−O−C deformation, which suggests a decrease in the bond order, indicating an interaction between the ionic liquid and the polymer. This interaction and the disappearance of the melting transition of the ionic liquid and the change of T_g observed in the DSC measurements indicate that the components of polymer gel electrolyte are miscible (46, 47).

Further evidence of this interaction is shown in the ^{1}H NMR spectra (Figure 3). The observation of the interaction between the imidazolium cation and ether units in solid-state samples using NMR spectroscopy can be difficult, because the intermolecular interactions are very intense and can lead to complex and broad signs, with low resolution. Therefore, investigations in a solvent medium can make the visualization easier.

In the pure MPII spectra (Figure 3), the signal at 9.90 ppm can be attributed to the most acid proton in the imidazolium ring (located in position 1, see imidazolium cation structure in the inset in Figure 4). This peak is shifted to the weak field when the ionic liquid is mixed with the copolymer, indicating interaction between hydrogen 1 and the oxygen from the copolymer ether units. This shift is more pronounced for the mixture containing a higher amount of polymer (20 wt % MPII) as a consequence of the increase in the basicity of the medium, because of the increase in oxygen content for an increased copolymer concentration.

The signal attributed to the hydrogen atoms located in position 3 and 4 (doublet at 7.58 and 7.52 ppm for pure MPII), on the other hand, presents a shift in the opposite direction, toward the strong field. This also suggests that the oxygen atoms interact with the hydrogen in position 1, and the decrease of the resonance in the imidazolium cation provided by this hydrogen bond increases the eletronic density between the carbons located in position 3 and 4

Table 1. Parameters Obtained by Fitting the Nyquist Plots Depicted in Figure 6, Using the Equivalent Circuit $R_S[C(R_{CT}O)]$; Values for the Diffusion Coefficient Estimated Using eq 1 Are Also Shown

				O		
samples	R_S (Ω cm^2)	R_{CT} (Ω cm^2)	C (μF cm^2)	Y_0 (S)	B (s$^{1/2}$)	D (I_3^-) (cm^2 s^{-1})
70% MPII	48.0	11.4	8.45	0.4086	13.74	1.9×10^{-7}
40% MPII	90.1	39.1	10.86	0.1344	20.33	8.7×10^{-8}

(e.g., displacement to the strong field). Campbell and Johnson (48) observed a similar effect after addition of Cl^- ions to samples containing the imidazolium cation, and the opposite effect after decreasing the pH of the medium. Dinares and coworkers (49) observed the same effect after addition of oxyanions (increasing the basicity of the medium), in agreement with the results obtained in this work.

Electrochemical Measurements. The Nyquist diagrams of the electrolytes containing 40 and 70 wt % of MPII are presented in Figure 4. The response at high frequencies (1×10^6 to 1×10^1 Hz) can be attributed to the Pt| electrolyte interface, while the response at low frequencies can be associated with the diffusion processes in the electrolyte (50). An equivalent circuit (also shown in Figure 4) represented by $R_S[C(R_{CT}O)]$, was used to fit the EIS data. In this circuit, R_S and R_{CT} describe the resistance; O is intrisically related to the parameters Y_O and B, obtained from the fit, and accounts for a finite-length Warburg diffusion (Z_{Dif}), and C is the constant phase element, CPE. This circuit has been successfully employed to fit the data for polymer electrolytes (5, 50), liquid electrolytes (51) and ionic liquid-based electrolytes (52).

As shown in previous works (50, 53), the apparent diffusion coefficient of the ionic species can be roughly estimated as described in eq 1:

$$D = \frac{d^2}{B^2} \tag{1}$$

where the diffusion length, d, can be considered as the distance between the two electrodes.

This relation is obtained by eq 2

$$Z_{Dif} = R_{Dif}\{[\tanh(j\omega\tau)^{1/2}]/(j\omega\tau)^{1/2}\} \tag{2}$$

where the impedance of the Warburg diffusion in a finite-length region of length d (the thickness between the electrodes) can be expressed in terms of R_{Dif}, related as $R_{Dif} = B/Y_0$, and τ, described as $\tau = B^2 = d^2/D$ (54).

All the parameters estimated from the Nyquist plots using this equivalent circuit are described in Table 1. To reach equilibrium during charge transport across the cell, it is necessary to have the same D for the cation and the anion, and this was assumed in this work. Also, it has been proposed that at high concentration of I^-, the diffusion impedance is limited by the I_3^- diffusion (51); therefore, the D values estimated here are attributed to the apparent diffusion of triiodide ($D_{I_3^-}$).

The results obtained from the EIS investigation revealed a significant decrease in the overall impedance after increasing the amount of MPII. The estimated D values increased from 8.7×10^{-8} to 1.9×10^{-7} cm^2 s^{-1} when the amount of MPII was increased from 40 to 70 wt %, respectively. The higher content of P(EO-PO) (and consequently, the lower concentration of ionic species) in the electrolyte containing 40 wt % MPII contributed to the decrease in $D_{I_3^-}$ values. Nazmutdinova and coworkers (52) used the same procedure to estimate the diffusion coefficient in electrolytes based on a mixture of MPII and another ionic liquid and reported values of the same order of magnitude (1×10^{-7} cm^2 s^{-1}). For pure MPII, the diffusion coefficient of I_3^- was estimated to be 1.5×10^{-7} cm^2 s^{-1} (52), similar to the value found in this work for the electrolyte containing 70 wt % MPII. These values suggest that in the electrolyte with low polymer content, the diffusion of ionic species has a similar behavior as the diffusion in the pure ionic liquid. Also, under these conditions, is expected that all the ionic species are effectively dissociated in the polymer matrix. It should be pointed, however, that even the pure ionic liquid presents a diffusion coefficient smaller than that estimated for LiI/I_2 in acetonitrile ($\sim 1 \times 10^{-5}$ cm^2 s^{-1}, using the same technique) (51), which can be attributed to the higher viscosity of MPII when compared to organic solvents.

Dye-Sensitized Solar Cells. Figure 5 shows the $I-V$ curves obtained for the DSSC assembled with the gel electrolytes containing P(EO-PO) and 40 or 70 wt % of MPII. These data set forth a clear enhancement in the photocurrent (I_{sc}) values when the amount of ionic liquid in the P(EO-PO) matrix is increased (I_{sc} increases from 8.96 to 12.92 mA cm^{-2} under irradiation of 100 mW cm^{-2}). This behavior was expected considering the increase in ionic conductivity and $D_{I_3^-}$ values, as discussed before. Moreover, this electrolyte

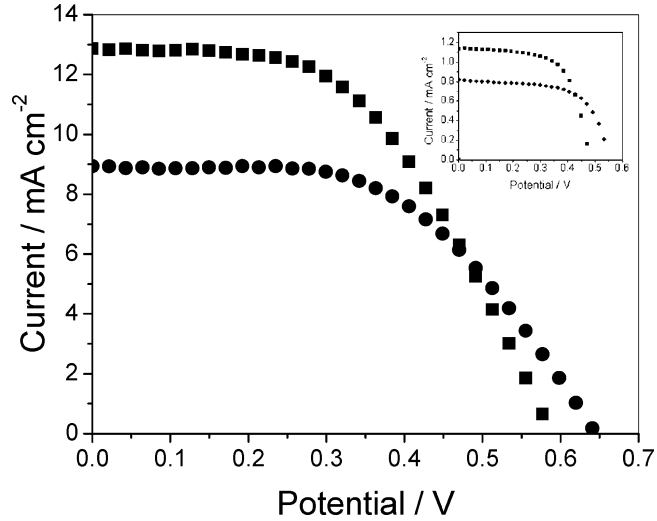

FIGURE 5. $I-V$ curves of DSSC assembled with polymer gel electrolytes of P(EO-PO) containing 40 (•) or 70 (■) wt % MPII, under irradiation of 100 mW cm^{-2}. The inset shows the curves obtained under 10 mW cm^{-2}.

contains more iodide ions, thus the regeneration of the oxidized dye is expected to be more efficient. The I_{sc} values obtained here are similar to the values reported for electrolytes based on ionic gel electrolytes (43, 55).

On the other hand, the high concentration of I_3^- and other polyiodides, as I_5^-, might also increase the dark current (recombination of the electrons injected in the TiO_2 with polyiodide ions in the electrolyte), reducing the V_{oc} values (V_{oc} decreased from 0.65 to 0.59 V under 100 mW cm^{-2}). Because I_2 forms I_3^- and other polyiodides, the donation of electrons to these species is favorable due the lower diffusion and higher electronic affinity (56). In a previous work, we reported that the presence of poly(ethylene oxide)-based copolymers in the electrolyte increases the values of V_{oc} because of the basic interaction between the oxygen atoms present in the polymer chains and the titania film (57). Thus, the lower V_{oc} values observed for the electrolytes containing 70 wt % MPII might also be due to the lower content of polymer in this electrolyte, which acts as a barrier inhibiting this recombination reaction. However, we cannot discard the possibility that the oxygen atoms from the polymer chains interact with the imidazolium cation (as discussed before), competing with the Ti(IV) sites. Singh and coworkers (27) and Wang and coworkers (26) also reported low values of V_{oc} for DSSC assembled with electrolytes containing MPII with PEO or poly(vinylidenefluoride-*co*hexafluoropropylene) (PVDF-HFP), respectively.

The DSSC assembled with the electrolyte containing 70 wt % MPII has 3.84 and 3.54% of efficiency, whereas the DSSC assembled with the electrolyte containing 40 wt % MPII presented efficiencies of 3.08 and 2.86% under 100 and 10 mW cm^{-2}, respectively. These results show that the performance of the DSSC containing ionic liquid is less dependent upon light intensity, similar to the behavior observed in DSSC with liquid electrolytes and opposed to the behavior usually observed for DSSC with polymer electrolytes (5, 7).

Figure 6 shows the $I-V$ curves obtained for DSSC assembled with the gel polymer electrolytes containing P(EO-PO) and 40 or 70 wt % of MPII, after addition of 20 wt % LiI. Table 2 summarizes the DSSC parameters obtained for all the electrolytes.

For the DSSC containing 70 wt % MPII, the effect of addition of LiI did not show improvements in I_{sc}, in agreement with the lower conductivity in this electrolyte. In this case, the high concentration of ionic species from the ionic liquid is expected to saturate the system; therefore, the LiI added may increase the formation of transient cross-linking points, reducing the free ions in the system. The DSSC assembled with 40 wt % MPII displayed a significant increase in the photocurrent after incorporation of LiI (from ~9 to 11 mA cm^{-2}). This is in agreement with the increase in the ionic conductivity observed for this electrolyte after addition of LiI because of the generation of more charge carriers.

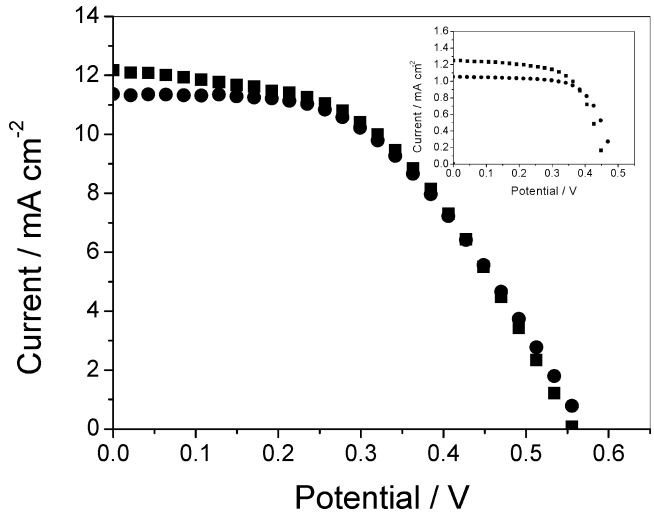

FIGURE 6. $I-V$ curves of DSSC assembled with polymer gel electrolytes of P(EO-PO) containing 40 (•) or 70 (■) wt % MPII, after addition of 20 wt % LiI, under irradiation of 100 mW cm^{-2}. The inset shows the curves obtained under 10 mW cm^{-2}.

On the other hand, in both cases, V_{oc} is reduced after addition of LiI due the higher concentration of I_3^-, increasing the recombination reaction between injected electrons and electrolyte. Also, we cannot discard the possibility of the intercalation of Li^+ ions into the TiO_2 structure, shifting down the Fermi level of this semiconductor (58, 59).

At low intensity, the electrolytes without LiI show solar cells with features of liquid electrolyte, less limited by mass transfer (higher efficiency at 100 mW cm^{-2}). Nevertheless, after addition of LiI, the solar cells present higher efficiencies at 10 mW cm^{-2} than the devices at 100 mW cm^{-2}, comparable to the typical behavior found when polymer electrolytes are employed (5, 7, 60). The insertion of LiI in the system could increase the transient cross-linking points, decreasing the kinetics of the dye regeneration reaction at 100 mW cm^{-2}. Thus, at low intensity, the mobility of the polymer chains and the redox species is enough to allow dye

Table 2. Performance of DSSC Employing Electrolytes of P(EO-PO) with 40 and 70 wt % MPII, with and without LiI, at 100 or 10 mW cm^{-2}

		electrolyte samples	V_{OC} (V)	I_{SC} (mA cm^{-2})	FF	η (%)
100 mW cm^{-2}	without LiI	70% MPII	0.59	12.92	0.51	3.84
		40% MPII	0.65	8.96	0.53	3.08
10 mW cm^{-2}		70% MPII	0.48	1.14	0.65	3.54
		40% MPII	0.56	0.82	0.63	2.86
100 mW cm^{-2}	with LiI	70% MPII	0.56	12.22	0.48	3.25
		40% MPII	0.57	11.38	0.49	3.17
10 mW cm^{-2}		70% MPII	0.46	1.25	0.64	3.66
		40% MPII	0.49	1.05	0.68	3.46

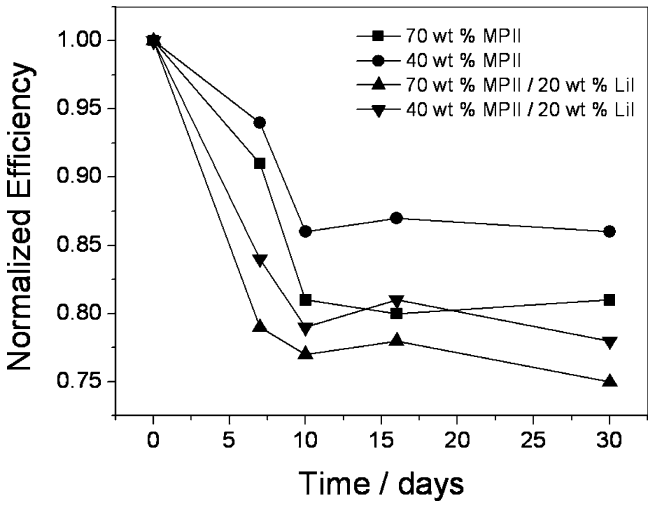

FIGURE 7. Variation in efficiency as a function of time for the DSSC assembled with polymer gel electrolyte of P(EO-PO) containing 40 or 70 wt % MPII, before and after addition of 20 wt % LiI. The solar cells were exposed to 100 mW cm^{-2} for 30 min each day.

cation regeneration more efficiently, whereas at full solar illumination, the electrolyte shows limited photocurrent by mass transfer (61, 62). The best efficiencies were observed for the electrolytes containing 70 wt % MPII, with and without LiI, in agreement with the higher ionic conductivity, $D_{I_3^-}$ and concentration of imidazolium cation observed for these electrolytes.

The whole set of results presented here indicate that the addition of LiI to the electrolytes can slightly improve the performance of the DSSC (since the increase was observed with 40 wt % MPII), but the addition of this material is not crucial, and the combination of only P(EO-PO) and MPII/I_2 as polymer gel electrolytes can lead to devices with promising efficiency. Figure 7 shows the stability of DSSC for a period of 30 days. We observed a decay in the performance after the first 10 days, reaching relative constant efficiencies after 20 days. For the devices using the electrolytes without LiI, the solar cells exhibit a better stability. It is interesting to note that the stability is remarkable for the devices with electrolytes containing 40 wt % MPII, if we compare to other solar cells. It seems that more ionic liquid less stable the device is. In general, the losses observed in all the devices are in agreement with the reported studies for polymer or gel electrolytes (13, 63, 64), showing an initial decay followed by a plateau of stability.

CONCLUSIONS

Polymer gel electrolytes based on the combination of poly(ethylene oxide-*co*-propylene oxide) and 1-propyl-3-methyl-imidazolium iodide were investigated. The interactions between the oxygen atoms present in the polymer chains and the imidazolium cation lead to high solubility and dissociation of the ionic liquid in the polymer medium, which is evidenced by DSC, FTIR, and ^{1}H NMR analysis. These high concentrations of free ions are responsible for the high ionic conductivity, reaching 2.4×10^{-3} S cm^{-1} for the system containing 70 wt % MPII. When LiI was added to this electrolyte, no significant effect was observed in the device's efficiency. Besides, the stability after 30 days is higher to electrolytes without LiI. The DSSC assembled with the electrolyte containing P(EO-PO) and 70 wt % ionic liquid exhibits an overall efficiency of 3.84% under 100 mW cm^{-2} and the solid-state nature of this system, even at high MPII concentration, is an advantage over DSSC assembled with liquid electrolytes or pure ionic liquid. The devices assembled using the polymer–ionic liquid mixture, where the concentration of this last component is 40 wt %, are more stable and this is an important information when considering the application of ionic liquids and their mixtures as electrolytes.

Acknowledgment. The authors thank CNPq and Fapesp for financial support and scholarships. The authors also acknowledge Daiso Co. Ltd. (Osaka) for supplying the copolymer used in this work and Prof. Carol H. Collins for English revision.

Supporting Information Available: FTIR analysis and schematic illustrations of the solar cell and the electrochemical cell used for the EIS measurements (PDF). This material is available free of charge via the Internet at http://pubs.acs.org.

REFERENCES AND NOTES

(1) O'Regan, B.; Grätzel, M. *Nature* **1991**, *353*, 737–740.
(2) Tan, S.; Zhai, J.; Xue, B.; Wan, M.; Meng, Q.; Li, Y.; Jiang, L.; Zhu, D. *Langmuir* **2004**, *20*, 2934–2937.
(3) Nogueira, A. F.; Longo, C.; De Paoli, M.-A. *Coord. Chem. Rev.* **2004**, *248*, 1455–1468.
(4) Ren, Y.; Zhang, Z.; Fang, S.; Yang, M.; Cai, S. *Sol. Energy Mater. Sol. Cells* **2002**, *71*, 253–259.
(5) Nogueira, V. C.; Longo, C.; Nogueira, A. F.; Oviedo, M. A. S.; De Paoli, M.-A. *J. Photochem. Photobiol., A* **2006**, *181*, 226–232.
(6) Nogueira, A. F.; De Paoli, M.-A. *Sol. Energy Mater. Sol. Cells* **2000**, *61*, 135–141.
(7) Nogueira, A. F.; Durrant, J. R.; De Paoli, M.-A. *Adv. Mater.* **2001**, *13*, 826–830.
(8) Longo, C.; De Paoli, M.-A. *J. Braz. Chem. Soc.* **2003**, *14*, 889–901.
(9) Benedetti, J. E.; De Paoli, M.-A.; Nogueira, A. F. *Chem. Commun.* **2008**, *9*, 1121–1123.
(10) Freitas, J. N.; Gonçalves, A. S.; Durrant, J. R.; De Paoli, M.-A.; Nogueira, A. F. *Electrochim. Acta* **2008**, *53*, 7166–7172.
(11) Priya, A. R. S.; Subramania, A.; Jung, Y.-S.; Kim, K.-J. *Langmuir* **2008**, *24*, 9816–9819.
(12) Nakade, S.; Kanzaki, T.; Wada, Y.; Yanagida, S. *Langmuir* **2005**, *21*, 10803–10807.
(13) Freitas, J. N.; Nogueira, A. F.; De Paoli, M.-A. *J. Mater. Chem.* **2009**, *19*, 5279–5294.
(14) Han, H. W.; Bach, U.; Cheng, Y. B.; Caruso, R. A. *Appl. Phys. Lett.* **2007**, *90*, 213510.
(15) Kim, Y. J.; Kim, J. H.; Kang, M.-S.; Le, M. J.; Won, J.; Lee, J. C.; Kang, Y. S. *Adv. Mater.* **2004**, *16*, 1753–1757.
(16) Hurley, F. H.; Wier, T. P. *J. Electrochem. Soc.* **1951**, *98*, 203–206.
(17) Wang, P.; Zakeeruddin, S. M.; Moser, J.-E.; Baker, R. H.; Grätzel, M. *J. Am. Chem. Soc.* **2004**, *126*, 7164–7165.
(18) Wang, P.; Wenger, B.; Baker, R. H.; Moser, J.-E.; Teuscher, J.; Kantlehner, W.; Mezger, J.; Stoyanov, E. V.; Zakeeruddin, S. M.; Grätzel, M. *J. Am. Chem. Soc.* **2005**, *127*, 6850–6856.
(19) Kuang, D.; Walter, P.; Nüesch, F.; Kim, S.; Ko, J.; Comte, P.; Zakeeruddin, S. M.; Nazeeruddin, M. K.; Grätzel, M. *Langmuir* **2007**, *23*, 10906–10909.
(20) Meng, Q.-B.; Takahashi, K.; Zhang, X.-T.; Sutanto, I.; Rao, T. N.; Sato, O.; Fujishima, A. *Langmuir* **2003**, *19*, 3572–3574.
(21) Fei, Z.; Kuang, D.; Zhao, D.; Klein, C.; Ang, W. H.; Zakeeruddin, S. M.; Grätzel, M.; Dyson, P. J. *Inorg. Chem. Commun.* **2006**, *45*, 10407–10409.
(22) Hanabusa, K.; Fukui, H.; Suzuki, M.; Shirai, H. *Langmuir* **2005**, *21*, 10383–10390.

(23) Li, D.; Wang, M.; Wu, J.; Zhang, Q.; Luo, Y.; Yu, Z.; Meng, Q.; Wu, Z. *Langmuir* **2009**, *25*, 4808–4814.
(24) Wang, P.; Zakeeruddin, S. M.; Comte, P.; Exnar, I.; Grätzel, M. *J. Am. Chem. Soc.* **2003**, *125*, 1166–1167.
(25) Papageorgiou, N.; Athanassov, Y.; Armand, M.; Bonhóte, P.; Pettersson, H.; Azam, A.; Grätzel, M. *J. Electrochem. Soc.* **1996**, *143*, 3099–3108.
(26) Wang, P.; Zakeeruddin, S. M.; Exnar, I.; Grätzel, M. *Chem. Commun.* **2002**, 2972–2973.
(27) Singh, P. K.; Kim, K.-W.; Park, N.-G.; Rhee, H.-W. *Synth. Met.* **2008**, *158*, 590–593.
(28) Wang, P.; Zakeeruddin, S. M.; Comte, P.; Exnar, I.; Grätzel, M. *J. Am. Chem. Soc.* **2003**, *125*, 1166–1167.
(29) Wang, P.; Zakeeruddin, S. M.; Moser, J. E.; Nazeeruddin, M. K.; Sekiguchi, T.; Grätzel, M. *Nat. Mater.* **2003**, *2*, 402–407.
(30) Bhattacharya, B.; Tomar, S. K.; Park, J.-K. *Nanotechnology* **2007**, *18*, 485711.
(31) Singh, P. K.; Kim, K.; Lee, J.; Rhee, H. *Phys. Status Solidi A* **2006**, *203*, R88–R90.
(32) Singh, P. K.; Kim, K.; Park, N.; Rhee, H. *Macromol. Symp.* **2007**, *162*, 249–250.
(33) Wang, M.; Xiao, X.; Zhou, X.; Li, X.; Lin, Y. *Sol. Energy Mater. Sol. Cells* **2007**, *91*, 785–790.
(34) Ohno, H. *Electrochim. Acta* **2001**, *46*, 1407–1411.
(35) Wang, M.; Yin, X.; Xiao, X. R.; Zhou, X. W.; Yang, Z. Z.; Li, X. P.; Lin, Y. *J. Photochem. Photobiol., A* **2008**, *194*, 20–26.
(36) Suzuki, K.; Yamaguchi, M.; Hotta, S.; Tanabe, N.; Yanagida, S. *J. Photochem. Photobiol., A* **2004**, *164*, 81–85.
(37) Li, N.; Zhang, S.; Li, X.; Yu, L.; Zheng, L. *Colloid Polym. Sci.* **2009**, *287*, 103–108.
(38) Bhattacharya, B.; Lee, J. Y.; Geng, J.; Jung, H.-T.; Park, J.-K. *Langmuir* **2009**, *25*, 3276–3281.
(39) Nakade, S.; Kanzaki, T.; Kambe, S.; Wada, Y.; Yanagida, S. *Langmuir* **2005**, *21*, 11414–11417.
(40) O'Regan, B.; Durrant, J. R.; Sommeling, P. M.; Bakker, N. J. *J. Phys. Chem. C* **2007**, *111*, 14001–14010.
(41) Fukui, A.; Komiya, R.; Yamanaka, R.; Islam, A.; Han, L. *Sol. Energy Mater. Sol. Cells* **2006**, *90*, 649–658.
(42) Benedetti, J. E.; Gonçalves, A. D.; Formiga, A. L. B.; De Paoli, M.-A.; Li, X.; Durrant, J. R.; Nogueira, A. F. *J. Power Sources* **2010**, *195*, 1246–1255.
(43) Kubo, W.; Murakoshi, K.; Kitamura, K.; Yoshida, Y.; Haruki, M.; Hanabusa, H.; Shirai, H.; Wada, Y.; Yanagida, S. *J. Phys. Chem. B* **2001**, *105*, 12809–12815.
(44) Kalaignan, G. P.; Kang, M.-S.; Kang, Y. S. *Solid State Ionics* **2006**, *177*, 1091–1097.
(45) Watanabe, M.; Ogata, N. In *Polymer Electrolyte Reviews*; Maccallum, J. R., Vincent, C. A., Eds.; Elsevier Science Publishers: London, 1989; Vol. 1, pp 39—51.
(46) Arunbabu, D.; Sannigrahi, A.; Jana, T. *J. Phys. Chem. B* **2008**, *112*, 5305–5310.
(47) Shi, J.; Peng, S.; Pei, J.; Liang, Y.; Cheng, F.; Chen, J. *ACS Appl. Mater. Interfaces* **2009**, *1*, 944–950.
(48) Campbell, J. L. E.; Johnson, K. E. *Inorg. Chem.* **1993**, *32*, 3809–3815.
(49) Dinarès, I.; Miguel, C. G.; Mesquida, N.; Alcalde, E. *J. Org. Chem.* **2009**, *74*, 482–485.
(50) Longo, C.; Nogueira, A. F.; De Paoli, M.-A.; Cachet, H. *J. Phys. Chem. B* **2002**, *106*, 5925–5930.
(51) Hauch, A.; Georg, A. *Electrochim. Acta* **2001**, *46*, 3457–3466.
(52) Nazmutdinova, G.; Sensfuss, S.; Schödner, M.; Hinsch, A.; Sastrawan, R.; Gerhard, D.; Himmler, S.; Wasserscheid, P. *Solid State Ionics* **2006**, *177*, 3141–3146.
(53) Girotto, E. M.; De Paoli, M.-A. *Quim. Nova* **1999**, *22*, 358–368.
(54) Macdonald, J. R. In *Impedance Spectroscopy*; Macdonald, J. R., Ed.; John Wiley: New York, 1987.
(55) Kubo, W.; Kambe, S.; Nakade, S.; Kitamura, T.; Hanabusa, K.; Wada, Y.; Yanagida, S. *J. Phys. Chem. B* **2003**, *107*, 4374–4381.
(56) Matsuda, T.; Matsumoto, H. *Electrochem.* **2002**, *70*, 446–448.
(57) Nogueira, A. F.; De Paoli, M.-A.; Montanari, I.; Monkhouse, R.; Nelson, J.; Durrant, J. R. *J. Phys. Chem. B* **2001**, *105*, 7517–7524.
(58) Enright, B.; Redmond, G.; Fitzmaurice, D. *J. Phys. Chem.* **1994**, *98*, 6195–6200.
(59) Redmond, G.; Fitzmaurice, D. *J. Phys. Chem.* **1993**, *97*, 1426–1430.
(60) Ito, B. I.; Freitas, J. N.; De Paoli, M.-A.; Nogueira, A. F. *J. Braz. Chem. Soc.* **2008**, *19*, 688–696.
(61) Kuang, D.; Klein, C.; Zhang, Z.; Ito, S.; Moser, J.-E.; Zakeeruddin, S. M.; Grätzel, M. *Small* **2007**, *12*, 2094–2102.
(62) Kuang, D.; Klein, C.; Ito, S.; Moser, J. E.; Humphry-Baker, R.; Evans, N.; Duriaux, F.; Grätzel, C.; Zakeeruddin, S. M.; Grätzel, M. *Adv. Mater.* **2007**, *19*, 1133–1137.
(63) Longo, C.; Freitas, J. N.; De Paoli, M.-A. *J. Photochem. Photobiol., A* **2003**, *159*, 33–39.
(64) Freitas, J. N.; Longo, C.; Nogueira, A. F.; De Paoli, M.-A. *Sol. Energy Mater. Sol. Cells* **2008**, *92*, 1110–1114.

AM900596X